Optimisation of bremsstrahlung recovery in $B^+ \to K^+e^+e^-$ decays for the LHCb Upgrade II

Angela Moskal, Federico Betti, and Sascha Stahl
(Dated: October 1, 2022)

This document is a preliminary assessment of the electromagnetic calorimeter (ECAL) timing resolution for LHCb upgrade II in preparation for the high luminosity LHC (HL-LHC). LHCb specializes in beauty physics to probe sources of matter-antimatter asymmetry in the universe. A process of interest for this sector is $B^+ \to K^+e^+e^-$ and it is for the low energy bremsstrahlung emitted during this decay that tuning of ECAL timing resolution is performed. This decay is rare, and while the HL-LHC is intended to illuminate such rare processes, it is also a challenge to mitigate the pile up and radiation damage that comes with such high luminosities. Currently in development for upgrade II is a robust ECAL with increased granularity and new spaghetti calorimeter (SpaCal) technology. All data analyzed in this study comes from a Geant4 Simulation of the upgrade II ECAL. We observe a drastic improvement in timing resolution, $\mathcal{O}(10)$ ps, for the new SpaCal technology as compared to the older Shashlik technology. We also show how timing precision improves for the more energetic photon showers and how the precision depends on where in the ECAL the signal is being registered. This study serves as a useful starting point for future bremsstrahlung recovery optimisation studies.

I. INTRODUCTION

In 2035, the LHC is expected to start Run 5, operating at a higher than ever luminosity of $1-2\times10^{34}$ cm^{-2}s^{-1}, with 2000 charged particles produced per bunch crossing [1]. This increase in statistics will illuminate rare processes, such as the decay $B^+ \to K^+e^+e^-$, improving the prospects for flavour physics studies at LHCb. Recent measurements of $B^+ \to K^+e^+e^-$ and $B^+ \to K^+\mu^+\mu^-$ decay rates have shown evidence for lepton universality violation, suggesting that new physics (NP) discoveries beyond the SM are within reach [2]. This high luminosity also imposes strict requirements on the LHCb detector if it is to fully exploit the flavour-physics opportunities presented by HL-LHC. Of focus in this paper is the electromagnetic calorimeter (ECAL) and the requirements it will need to satisfy to maintain performance. Firstly, radiation damage to the ECAL modules will need to be addressed as the ECAL for the ongoing run 3 will not survive the projected Run 5 radiation dose of 1 Mgy in the innermost region (see figure 1).

At this luminosity, mitigating pile up also becomes a challenge. The detector will need to perform at a maximum pileup of ~ 40 [1]. For the ECAL, this requires timing resolution on the order of 10 ps, increased granularity and denser absorber materials. The focus of this project is to look at the timing resolution of the future ECAL with the application of recovering bremsstrahlung photons produced in $B^+ \to K^+e^+e^-$ decay (shown in figure 2).

As the trajectories of the products from $B^+ \to K^+e^+e^-$ decay are curved by the magnetic field in the LHCb detector, bremsstrahlung photons are emitted. What is particularly unique about this study is the low energy regime of the bremsstrahlung photons. This energy regime hasn't yet been explored in the context of the ECAL group at LHCb and so the study of timing resolution and timing cuts needed to distinguish bremsstrahlung photons produced in $B^+ \to K^+e^+e^-$ from pile-up is an area of great interest.

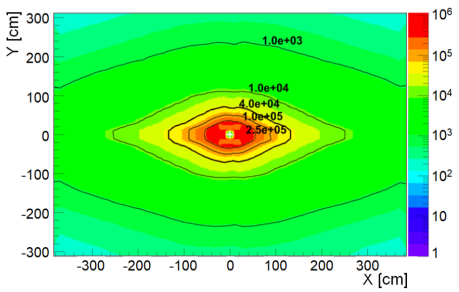

FIG. 1: ECAL projected accumulated radiation dose for Run 5.

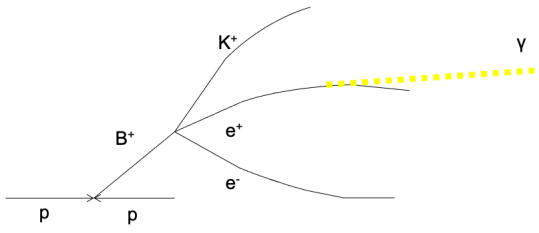

FIG. 2: A proton-proton collision producing a B meson which then undergoes the decay of interest for this study, $B^+ \to K^+e^+e^-$.

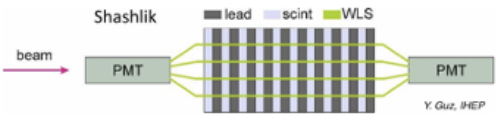

FIG. 3: Side view of the upgrade II shashlik electromagnetic calorimeter module.

A. Shashlik Electromagnetic Calorimeter

At the time of writing this paper, the ECAL at LHCb is composed of Shashlik calorimeter modules with only back readout. The geometry of the Shashlik module for Run 5 is shown in figure 3, with alternating tiles of scintillator and absorber material transverse to the beam direction as well as an additional front readout. Plastic is used for the scintillating material and lead is used for the absorber material [3]. Electromagnetic showers are generated in the lead absorber which excite the plastic scintillator. The resultant scintillation photons are picked up by wavelength shifting optical fibres (WLS) and guided to the front and back photomultiplier tubes (PMTs) where they are registered as a signal. The WLS fibres do not have sufficient radiation hardness to satisfy the Run 5 requirements for the innermost regions of the ECAL. This calls for a paradigm shift in module technology, introduced in the next section.

B. Spaghetti Calorimeter (SpaCal)

SpaCal modules are the proposed solution for a fast, radiation hard ECAL module. Its geometry, shown in figure 4, consists of a block of absorber with scintillating fibres running parallel to the beam direction, propagating a signal to front and back PMTs. In contrast to Shashlik, scintillating photons are produced directly in the fibres, eliminating the need for wavelength-shifting fibres, which are difficult to make radiation-hard [4]. The material choice depends on the module's placement in the ECAL. Looking back at figure 1, the innermost region, bombarded with the highest radiation dose, will have SPACAL modules made with tungsten absorber and garnet crystal fibres. Outwards, the SPACAL modules will instead be made with lead absorber and plastic scintillating fibres.

The currently proposed ECAL will have 6 distinct regions, with SPACAL modules populating the 2 innermost regions where radiation dose is highest, and Shashlik modules populating the outermost 4 regions. The size of the modules increases radially outwards so that the granularity will always be sufficient to distinguish neighbouring electromagnetic showers.

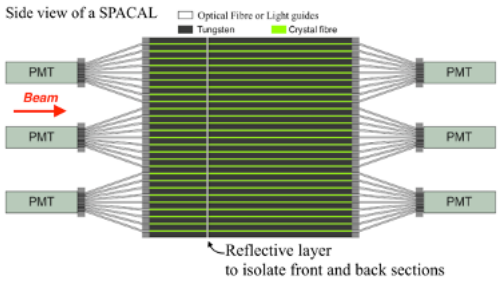

FIG. 4: Side view of SPACAL electromagnetic calorimeter module.

II. ANALYSIS

A. Simulation

In this physics study, particle flux from LHCb simulations is used as input. Ray tracing of cherenkov photons, mapping of energy deposition and parametrized transport of scintillation photons is carried out in Geant4 to simulate the photodetector response. Workflow is visualized in figure 5. Both the Shashlik and SPACAL modules are implemented and it is with this simulated data that analysis of timing resolution in the ECAL is performed.

B. Timing Resolution Analysis

In the ECAL, photon showers excite the scintillator which in turn emit scintillating photons. Depending on the technology, the scintillating photon will either be picked up by a WLS and carried to the PMTs or carried directly to the PMT via the scintillating fibre of origin. In any case, time will have elapsed between when the photon originally arrived at the scintillating material and when that event was registered as a signal by the PMT. We look at the distribution in time elapsed across many events in each region of the ECAL and for both front PMTs and back PMTs. Figure 6a is a typical time distribution for region 1 with the signal from the front PMT. The difference in Shashlik and SPACAL performance is made apparent in the timing distribution plots with all regions overlayed (figure 6b). SPACAL registers the signal an average of 2ns earlier than Shashlik due to the scintillating photons being produced directly in the optical fibres rather than needing to be first picked up by WLS fibres. The time resolution is quantified by the standard deviation (σ_t) of the gaussian fit to the timing distribution.

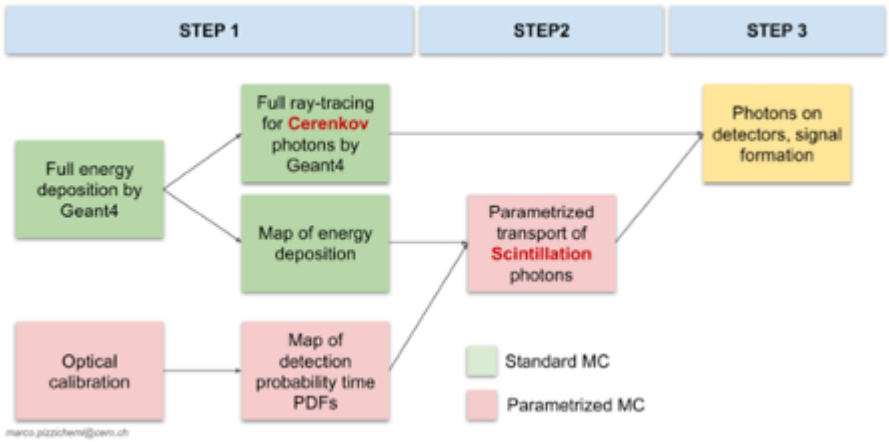

FIG. 5: Visualization of workflow involved in data simulation

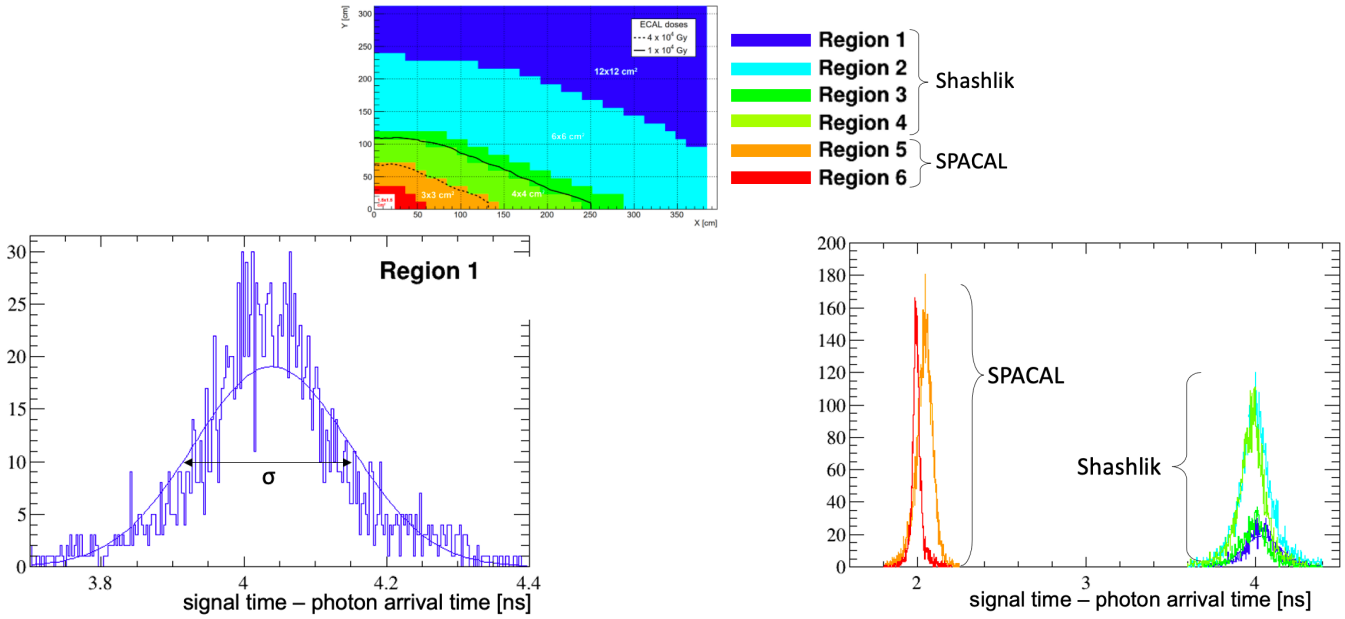

(a) Region 1 with a gaussian fit.

(b) All regions.

FIG. 6: Distribution of time elapsed between photon arrival and signal generation in the front PMT.

The Geant4 simulation also gives the energy for each electromagnetic shower. Figure 7 shows a typical energy distribution along with boundaries that split the histogram into 9 equally sized bins.

Energy constraints are imposed on the timing distribution plots to observe trends in timing resolution across energy ranges (see figure 8). It should be noted that the energy constraints are defined with respect to the response from the back PMTs, so it is not necessarily true that those same energy constraints split the energy distribution coming from the front PMT into equally sized bins.

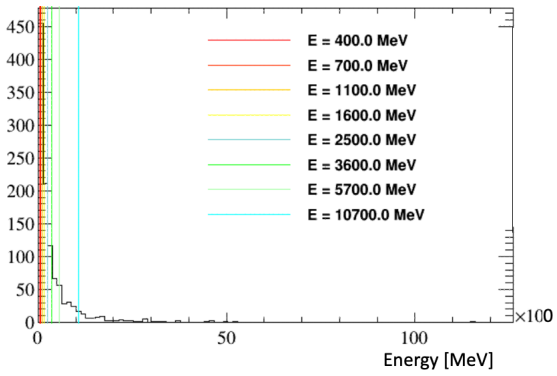

FIG. 7: Energy distribution of a photon shower in region 1, frontal PMT response.

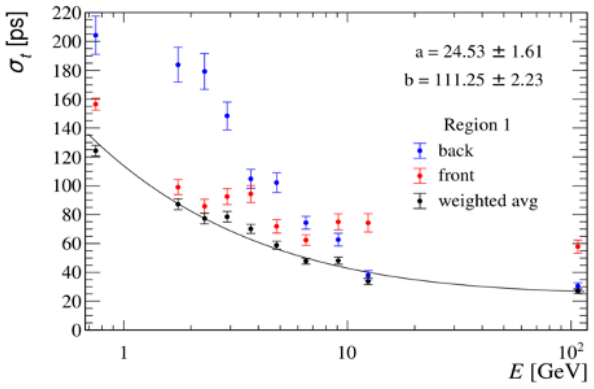

(a) Region 1

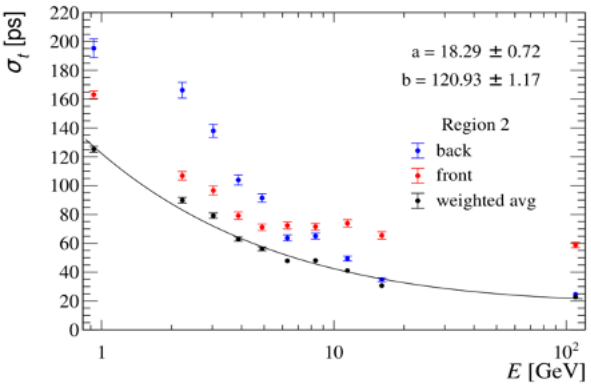

(b) Region 2

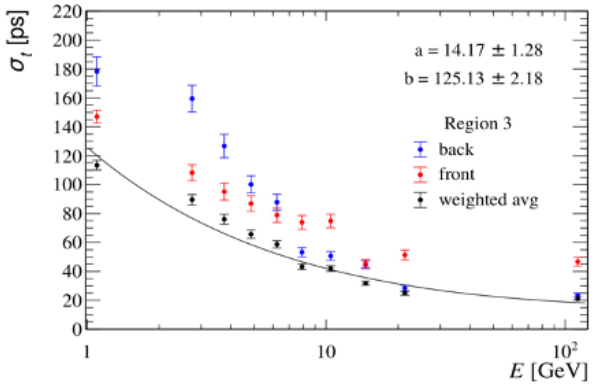

(c) Region 3

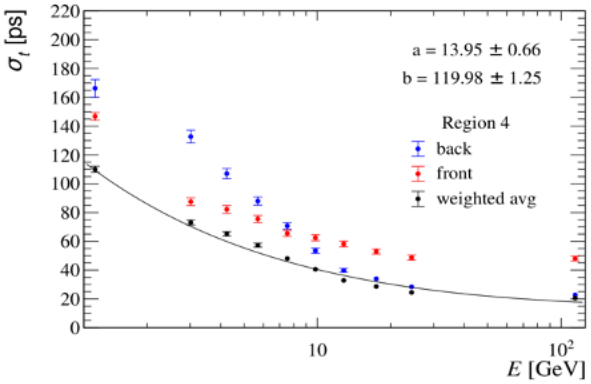

(d) Region 4

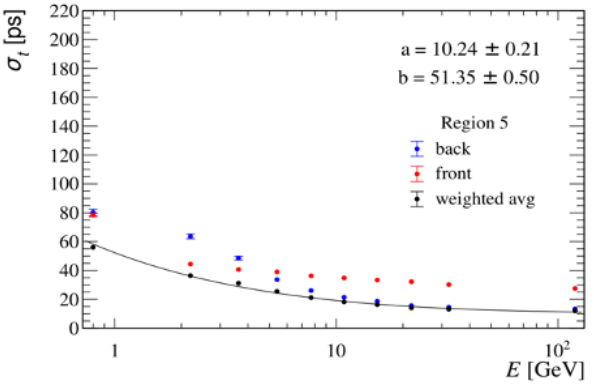

(e) Region 5

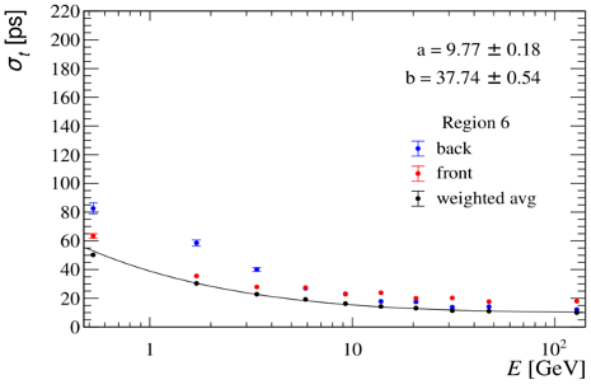

(f) Region 6

FIG. 8: Timing resolution versus energy. Front PMT response in red and back PMT response in blue. A weighted average of both PMTs is shown in black. The fitting function for the weighted average is $\sigma_t = \sqrt{a^2 + b^2/E}$ with a and b as fitting parameters.

What we see is a decrease in σ_t (i.e. better timing resolution) as the energy increases. This trend is true for all regions and both front and back PMTs. We perform a weighted average of σ_t from the front and back PMTs to obtain a curve that is empirically described by $\sigma_t = \sqrt{a^2 + b^2/E}$ where a corresponds to the energy resolution in the high energy range while b dominates at low energies. At low energy ranges, the front PMT gives better timing resolution, but at some energy (5-9 GeV), there is a cross over and the back PMT begins to perform better. This is attributed to the fact that higher energy electromagnetic showers penetrate deeper into the ECAL, closer to the back PMTs. The vertical axis has been made consistent across regions to highlight the fact that the timing resolution improves for centrally located regions. Again, the difference in Shashlik and SPACAL performance is made evident by the marked jump in timing resolution between regions 5/6 and regions 1-4. A

more subtle improvement in timing resolution between region 5 and 6 is attributed to region 6 having shorter fibres. All plots in Figure 8 can be further improved by fine tuning the energy bin boundaries and the fitting range for the timing distribution within each energy bin.

III. CONCLUSION

In this study, we have made a preliminary assessment of the ECAL timing resolutions for low energy range bremsstrahlung photon recovery in the decay $B^+ \to K^+e^+e^-$. This was done for both Shashlik and SPACAL ECAL modules and across a range of energies lower than what has been explored in the LHCb ECAL group thus far. When we begin to look at data sets that include pile-up, these timing resolutions can be used to establish suitable timing cuts.

Currently undergoing beam testing are Shashlik modules with faster WLS fibres than those implemented in the Geant4 simulation. The next steps would be to incorporate these changes into the simulation and carry out analysis of the simulated data with realistic transverse energy cuts on the photon shower clusters (25-50 MeV). Once the recovery of bremsstrahlung from $B^+ \to K^+e^+e^-$ is optimized in simulation, actual observation of these rare decays can be reliable made in Run 5 to probe physics beyond the SM [2].

[1] *Framework TDR for the LHCb Upgrade II (CERN-LHCC-2021-012)* (2021).

[2] R. Aaij (LHCb collaboration), Test of lepton universality in beauty-quark decays, e-print arXiv:2103.11769 www.nature.com/articles/s41567-021-01478-8.

[3] S. Barsuk (CERN), Design and construction of electromagnetic calorimeter for lhcb experiment, http://cds.cern.ch/record/691508 (2000).

[4] M. Lucchini, Test beam results with luag fibers for next-generation calorimeters, JINST **8**.